

# Bend Testing of Silicon Microcantilevers from 21°C to 770°C

DAVID E.J. ARMSTRONG<sup>1,2</sup> and EDMUND TARLETON<sup>1</sup>

1.—Department of Materials, University of Oxford, Oxford, UK. 2.—e-mail: David.armstrong@materials.ox.ac.uk

The measurement of mechanical properties at the microscale is of interest across a wide range of engineering applications. Much recent work has demonstrated that micropillar compression can be used to measure changes in flow properties at temperatures up to 600°C. In this work, we demonstrate that an alternative microscale bend testing geometry can be used to measure elastic, plastic, and fracture behavior up to 770°C in silicon. We measure a Young's modulus value of 130 GPa at room temperature, which is seen to drop with increasing temperature to  $\approx 125$  GPa. Below 500°C, no failure is seen up to elastic strains of 3%. At 530°C, the microcantilever fractures in a brittle fashion. At temperatures of 600°C and above plastic deformation is seen before brittle fracture. The yield stresses at these temperatures are in good agreement with literature values measured using micropillar compression.

## INTRODUCTION

The development of microscale mechanical testing of focused ion beam (FIB) machined elements has come a long way since the initial work by Uchic et al.<sup>1</sup> Although the majority of reported work has focused on the compression of microscale and nanoscale pillars,<sup>2–5</sup> there has also been a substantial body of work based on the bending of microscale FIB-machined cantilevers in a wide range of materials systems.<sup>6–10</sup> Such microscale cantilever bend experiments have several advantages. First, as demonstrated by Gong and Wilkinson<sup>11</sup> and Armstrong et al.,<sup>12</sup> they can be used to accurately determine the elastic modulus of metals including copper and titanium with sufficient accuracy to allow the anisotropy in Young's modulus to be measured, without the need for finite-element modeling. In comparison, Young's moduli values measured from compression tests tend to significantly underestimate the elastic modulus unless the punch in effect from the pillar and any taper and misalignment is accounted for during modeling. If the elastic modulus extracted from the stress–strain curve is not accurately measured, then it stands to reason that either the stress or strain is incorrectly reported. Second, bend samples can be notched—either by FIB machining<sup>13</sup> or by other means such as using a sharp prenotch,<sup>14</sup> which allows the measurement of fracture toughness of

either bulk materials<sup>8,10,14</sup> or of individual microstructural features such as phase interfaces<sup>15</sup> or grain boundaries.<sup>13</sup> Recent work by Jaya et al.<sup>16</sup> has shown that this microcantilever method produces fracture toughness values in silicon, which are in good agreement with fracture toughness values measured by other microscale means such as pillar splitting or double-edge-clamped beams as well as experimentally measured bulk fracture toughness values. Although micropillars have been tested to failure by compression in a range of brittle materials,<sup>17,18</sup> this does not allow the fracture toughness to be measured. In some cases, the geometry promotes the plastic flow of otherwise brittle materials,<sup>18,19</sup> and in others splitting is observed where cracks propagate through the sample.<sup>20</sup>

Although much microcantilever bending work has been carried out, it is almost exclusively reported at room temperature. In many engineering systems of interest, from aerospace to nuclear, the performance of the materials at temperature close to or above service conditions is vital to allow safe engineering design. In recent years, there has been a major effort by both equipment manufacturers and users to develop high-temperature nanoindentation and microscale deformation experiments. Most of this work has focused on either straightforward nanoindentation, for which nanohardness and indentation modulus have been reported up to

750°C.<sup>21–25</sup> For high-quality nanoindentation experiments to be performed, it is necessary to accurately know the area function for the indenter tip. As discussed by Wheeler et al.,<sup>23,26</sup> high-temperature experiments can quickly blunt indenter tips whether made from diamond or another hard material such as cubic boron nitride. Second, reactions can occur at high temperatures between samples and tips<sup>27</sup> (such as diamond dissolving in strong carbide formers such as tungsten or vanadium). This results in a rapid change in area functions and calibration must be performed regularly throughout the experimental procedure. Finally at higher temperatures, pile up effects may become more pronounced, resulting in a loss of tip calibration. As such, most high-temperature work has focused on performing microscale compression tests on a range of engineering materials at temperatures up to 600°C,<sup>28</sup> where tip damage is mitigated as wear to the flat punch is negligible.

In this work, we will demonstrate the testing of microcantilevers at temperatures from 21°C to 700°C in vacuum to measure the elastic modulus, yield stress, and fracture behavior in single-crystal silicon. The values measured are in good agreement with literature data.

### BEND TESTS IN SILICON

The microcantilevers were manufactured in an undoped single-crystal silicon (100) surface with the long axis of the cantilever in the  $\langle 001 \rangle$  direction (Fig. 1a). A Zeiss Auriga Dual Beam FIB-scanning electron microscope (SEM) (with Ga<sup>+</sup> ions; Carl Zeiss, Oberkochen, Germany) was used to manufacture the microcantilevers following the method described by Armstrong et al.<sup>12</sup> The final cantilevers had a length of  $\approx 27 \mu\text{m}$ , a width of  $\approx 4 \mu\text{m}$ , a triangular cross section with a maximum depth

of  $\approx 5 \mu\text{m}$  (Fig. 1b). Each cantilever was imaged using the SEM column of the Auriga FIB-SEM before testing for accurate measurement of the test geometry and afterward to study the deformation that had occurred.

Testing was performed in a NanotestXtreme (MML Ltd., Wrexham, U.K.), nanoindenter housed in a vacuum chamber (Fig. 2a). The chamber was purged with argon prior to being evacuated to a vacuum level of  $1 \times 10^{-5}$  mbar prior to testing and was held at this level for all experiments.

A cubic boron nitride Berkovich indenter was used, which was independently heated from the samples. The samples were mounted on a hot stage using Forta Fix Autostic FC6 high-temperature cement (Fig. 2b) with thermocouples mounted inside the furnace to monitor furnace temperature and a second thermocouple mounted using the same cement on the sample surface to allow accurate matching of the sample surface and indenter temperature. The same method used by Gibson et al.<sup>21</sup> was used to match the sample and indenter temperature, which minimized the drift rates during the experiment. Figure 3 shows displacement versus time for constant load for two tests; in the first, the temperatures of the tip and sample have been matched, and in the second, they have been intentionally unmatched. This demonstrates the importance of ensuring isothermal contact; when the sample and indenter temperatures are matched, the drift rate is minimal across a 60-s hold period, with a 10°C difference in temperature over 100 nm of drift are observed. To ensure accurate placement of the indenter tip on the microcantilever, each sample was imaged by scanning the indenter tip across the surface with a small ( $\approx 1 \mu\text{N}$ ) load to produce a surface profile image (Fig. 4) with surface height data collected every 0.25  $\mu\text{m}$ .

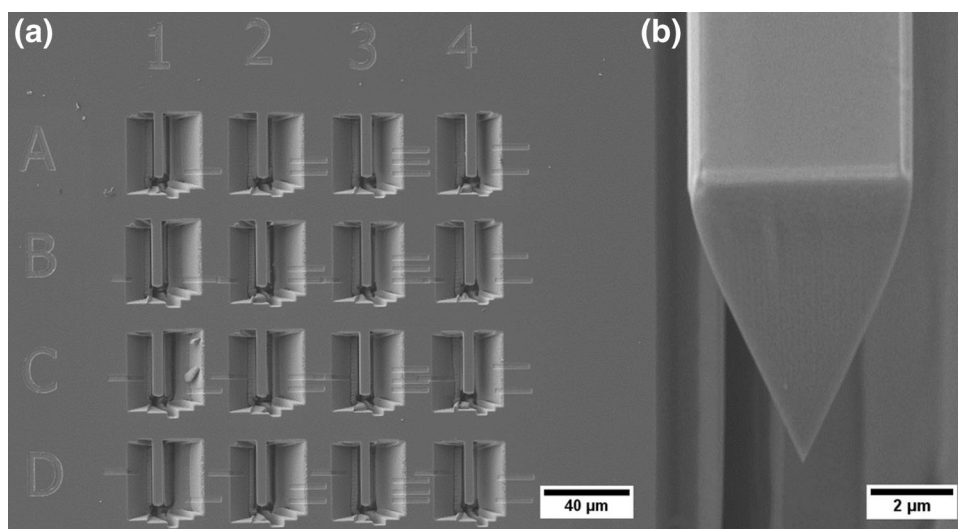


Fig. 1. (a) Array of microcantilevers manufactured in single-crystal silicon prior to testing. (b) Single cantilever tilt showing end geometry (tilt corrected).

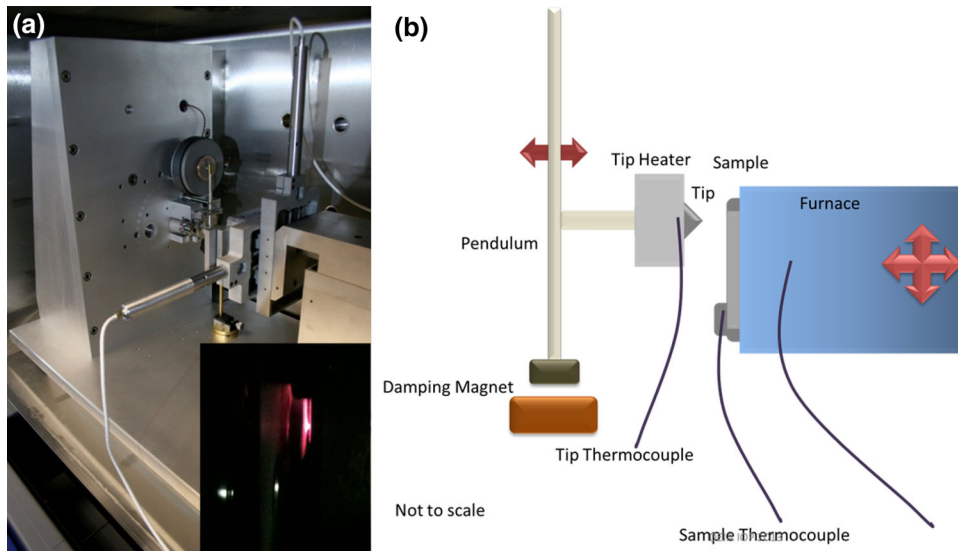


Fig. 2. (a) Internal layout of nanoTestExtreme; inset shows tip in heat shield at 700°C. (b) Schematic of test layout showing thermocouple positions for matching of tip and sample temperatures.

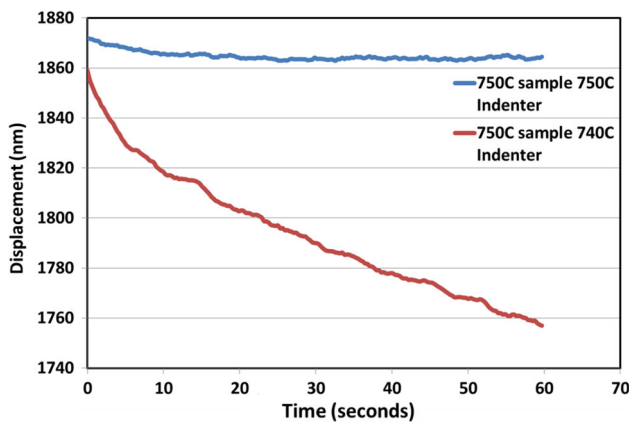


Fig. 3. Time–displacement data at peak load for two tests showing the importance of isothermal contact.

The indenter tip was then placed close to the free end of the cantilever and the load applied. A constant loading rate of 0.05 mN/s was used with a maximum displacement of between 1000 nm and 3000 nm (Fig. 5).

Figure 4 shows the surface scans of the micro-cantilevers up to 770°C, collected using the same parameters. Although some small scan artefacts can be seen at higher temperatures, the cantilever can be clearly identified for testing in each case.

Figure 6 shows the stress–strain curves calculated from the raw-load displacement data using simple beam theory (as described in Armstrong et al.<sup>12</sup>). A small amount of hysteresis is seen in the load–unload curves at lower temperatures due to plastic deformation under the sharp indenter tip as previously seen in other work.<sup>12</sup> The Young’s modulus values calculated are shown in Table I, alongside the literature values taken from Ref. 29. The

Young’s modulus values are seen to be consistently low compared with the literature values. As described by Gong and Armstrong,<sup>11,12</sup> this is due to the flexure of the top surface of the fixed end of the cantilever where it is not truly encastred. To account for this, finite-element analysis (FEA) was conducted using a simple elastic model (Fig. 7) to fit to the load–displacement data, which takes into account deformation in the fixed end of the cantilever. The values from Table I are in good agreement with the literature values, which show only a small drop ( $\approx 10$  GPa) across the temperature range used.

The cantilevers tested up to 530°C showed pure elastic deformation with no plasticity evident in the load displacement curve. Figure 8a and b shows the surface profile scans of a cantilever tested at room temperature before and after testing; no permanent deformation of the cantilever is observable. At 530°C, a change in deformation was observed. Although elastic deformation was observed initially, at a stress of 2.8 GPa the cantilever catastrophically fractured seen by the sudden displacement burst and near vertical unloading section. At 600°C, a further change in deformation mechanism is observed; significant plasticity is observed above a stress of 2.7 GPa to a maximum load of 3.7 GPa at which load fracture again occurs. This fracture was confirmed by a surface profile scan made immediately after testing (Fig. 8c and d) and subsequently in the secondary electron image (Fig. 9a), showing that the cantilever is no longer present in the test position and through fracture has occurred. At 770°C, similar behavior was observed with a lower yield stress of 1.6 GPa followed by fracture occurring at 1.9 GPa. To confirm that plastic deformation rather than stable crack growth occurred, an interrupted test was performed at 770°C. The test

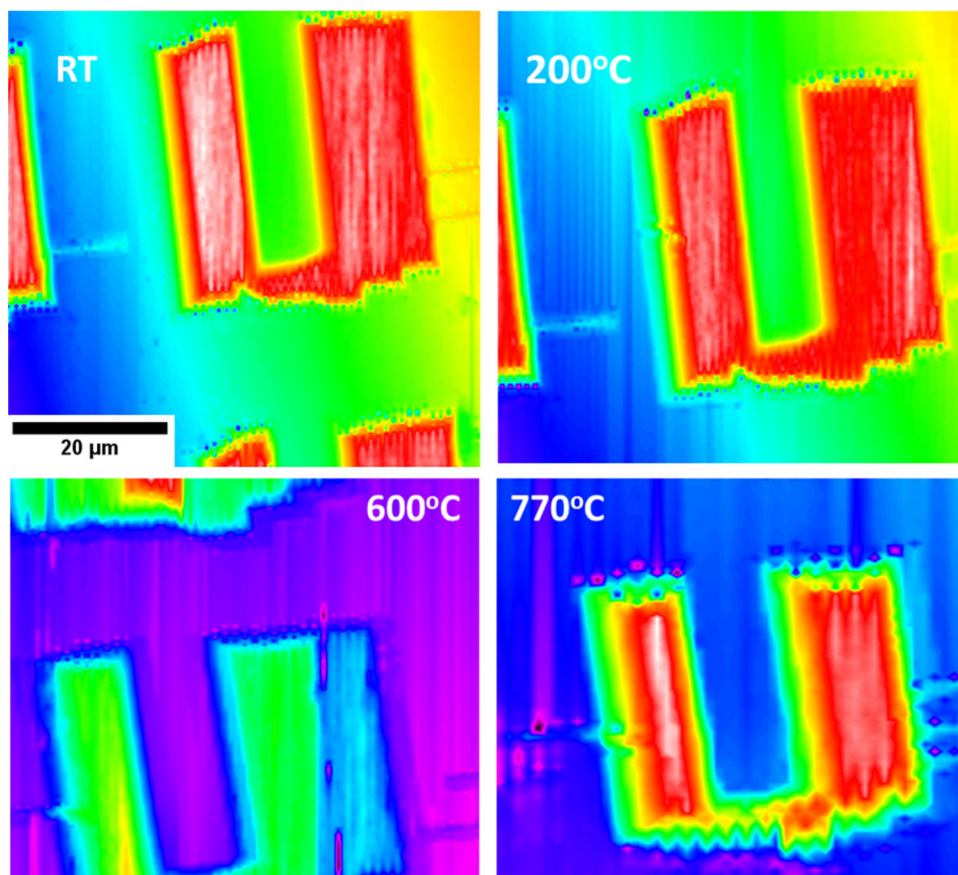


Fig. 4. Surface profilometry images of microcantilevers taken from room temperature to 770°C (RT = room temperature).

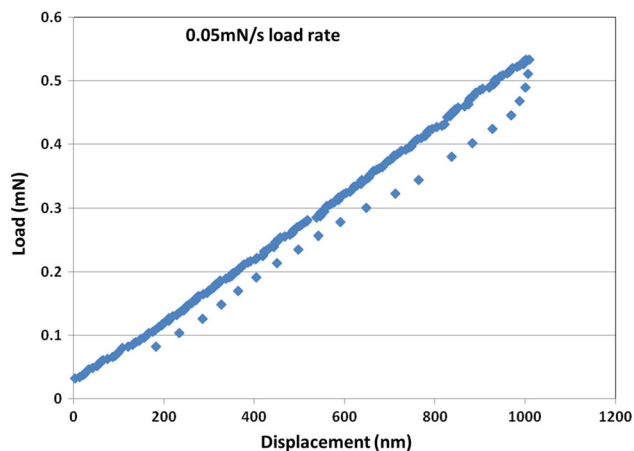


Fig. 5. Load–displacement curve of microcantilever at room temperature showing elastic deformation to 1000-nm deflection.

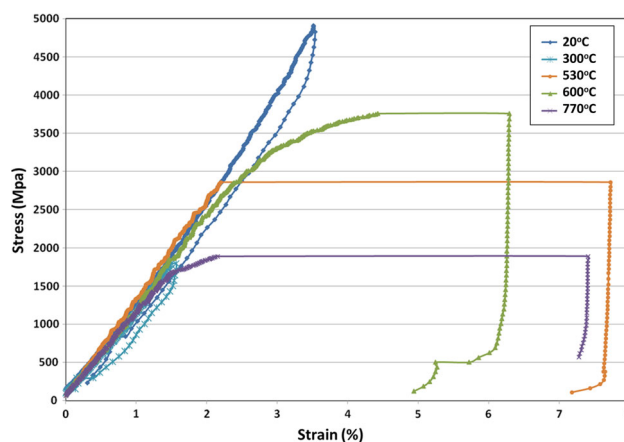


Fig. 6. Stress–strain curves calculated using simple beam theory for tested microcantilevers from 20°C to 700°C.

was interrupted after yield had occurred but before failure of the cantilever by fracture. This can be seen in Fig. 9b. Slip bands on the sample are clearly seen in the inset of the figure running across the width of the microcantilever, clearly showing that plastic deformation is occurring in silicon at these temperatures on the expected  $\langle 111 \rangle$  planes.

These data can be looked at in relation to other data in the literature regarding the high-temperature deformation of silicon. Pearson et al. studied the fracture behavior of 20- $\mu\text{m}$  diameter high-purity silicon whiskers from room temperature to 800°C. Below  $\approx 600^\circ\text{C}$ , the samples deformed elastically followed by brittle fracture, and above 600°C the samples underwent a small amount of plastic

**Table I. Young's Modulus as a Function of Temperature**

Temperature (°C)	Young's modulus literature value (GPa)	Young's modulus calculated using simple beam theory (GPa)	Young's modulus calculated using FEA (GPa)
21	130	110	130
200	128	105	128
300	126	109	129
530	122	105	126
600	121	110	131
770	120	105	125

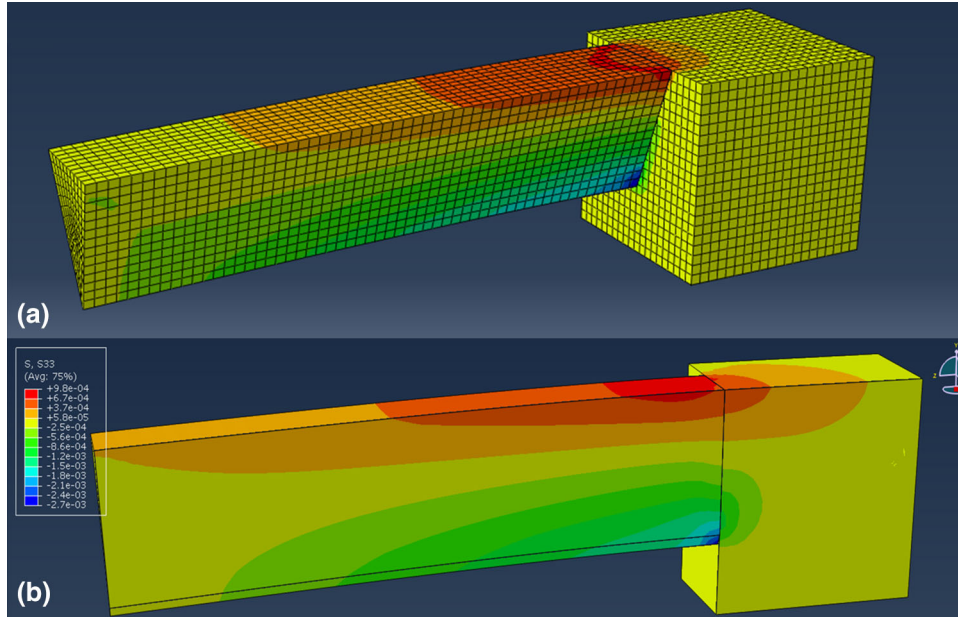


Fig. 7. (a) Finite-element model of microcantilever including fixed end showing mesh (b) cut through central line of model showing peak stress distribution at maximum deflection.

deformation before brittle failure and above 650°C significant plastic deformation was observed. This transition in behavior is in good agreement with the work of Hirsch and Roberts,<sup>30</sup> who studied the brittle-to-ductile transition in notched silicon samples of  $\approx 1 \text{ mm}^2$  cross-sectional area, tested in a four-point bend. They observed a transition that was logarithmically dependent on the strain rate of testing, with brittle-to-ductile transitions occurring between 550°C and 700°C.

More recently, several high-temperature micro-compression experiments have been performed on silicon pillars, with which the data in this study can be compared. Korte et al.<sup>31</sup> used an experimental setup similar to that used in this study to compress FIB prepared micropillars from room temperature to 500°C with a  $\langle 100 \rangle$  pillar normal direction. They found that there was a pronounced effect of both temperature and size on the failure behavior and yield stress. Although large diameter (typically 4000 nm) failed in a brittle manner by reducing the diameter to less than 1000 nm, plastic deformation occurred at room temperature. When the

temperature of compression of 2000-nm diameter pillars was increased from 25°C to 500°C, a transition was seen from a fracture-based failure mechanism (at a  $\approx 6 \text{ GPa}$ ) to a splitting mechanism. This mechanism had limited plasticity at 200°C at similar stress levels. Finally, full plastic deformation was observed at 500°C, with a yield stress of  $\approx 3 \text{ GPa}$ . Wheeler et al.<sup>27</sup> observed a transition in lithographically prepared pillars (also with a  $\langle 100 \rangle$  orientation), which failed catastrophically up to 100°C, to a splitting mechanism between 200°C and 300°C followed by plastic flow at  $\approx 400^\circ\text{C}$ . Wheeler's and Korte's values of yield stress of between 3 GPa and 4 GPa are higher than the values measured in this work (1.6–1.9 GPa). This discrepancy could be for several reasons, including the differences in size between the pillars and cantilevers, manufacturing methods, and the difference in loading modes between pure compression and bending. In particular, the bending deformation will promote the propagation of any cracks due to defects in the tension side of the cantilever induced in the manufacturing process. Rabier et al.<sup>32</sup> looked at several

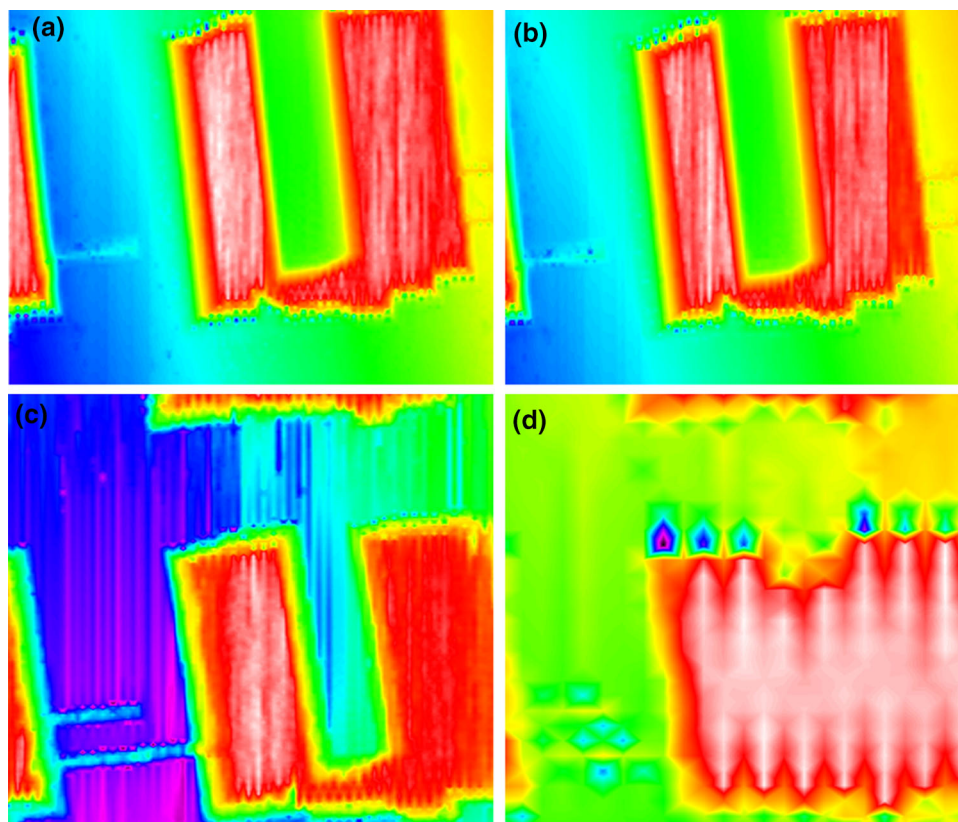


Fig. 8. Surface profile scans (a) room temperature before testing, (b) room temperature after testing, (c) 600°C before testing, and (d) 600°C after testing. No permanent deflection of the cantilever is seen after testing at room temperature, indicating that the deformation is purely elastic, whereas fracture has clearly occurred in the 600°C test.

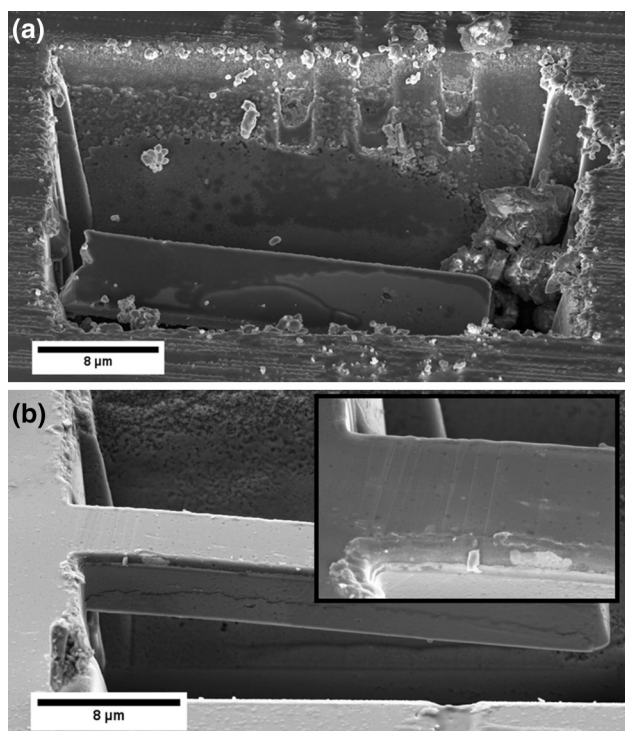


Fig. 9. (a) Microcantilever tested at 600°C to fracture. (b) Microcantilever tested at 770°C to yield and stopped before fracture.

different sized micropillars manufactured by FIB machining, oriented in a  $\langle 123 \rangle$  direction to ensure single-slip system activation. Again, larger pillars (2000-nm diameter) showed cracking and splitting, whereas smaller pillars (980 nm diameter) showed plastic flow even at room temperature. In these smallest pillars, the yield stress dropped from  $\approx 7$  GPa at 25°C to  $\approx 3$  GPa at 400°C.

The trend in the data for yield stress and critical temperature for change in deformation behavior measured using both macroscopic methods and microcompression testing are in good agreement with the yield stress behavior with increasing temperature and transition temperature values measured in this study. These microscale bend tests have advantages in probing true brittle behavior as the tensile side promotes true crack growth rather than a complex pillar splitting mechanism seen in compression testing. However, the differences in yield stresses measured at elevated temperatures need further study as to their controlling mechanisms.

## CONCLUSION

This study has shown that microcantilever experiments can be performed at temperatures up to 770°C; the measured values for the elastic,

plastic, and fracture behavior of single-crystal silicon are in good agreement with data in the literature from both bulk and microscale testing methods. Further work will focus on applying these high-temperature microcantilever techniques on notched samples to allow fracture toughness values to be measured and understanding differences in behavior between compression and bend tests.

### ACKNOWLEDGEMENTS

DEJA acknowledges the Royal Academy of Engineering for a Research Fellowship. Some of the work was supported financially by the EPSRC under program Grant EP/H018921/.

### OPEN ACCESS

This article is distributed under the terms of the Creative Commons Attribution 4.0 International License (<http://creativecommons.org/licenses/by/4.0/>), which permits unrestricted use, distribution, and reproduction in any medium, provided you give appropriate credit to the original author(s) and the source, provide a link to the Creative Commons license, and indicate if changes were made.

### REFERENCES

- M.D. Uchic, D.M. Dimiduk, J.N. Florando, and W.D. Nix, *Science* 305, 986 (2004).
- J.R. Greer and J.T.M. De Hosson, *Prog. Mater. Sci.* 56, 654 (2011).
- E.M. Grieveson, D.E.J. Armstrong, S. Xu, and S.G. Roberts, *J. Nucl. Mater.* 430, 119 (2012).
- D. Kiener, P. Hosemann, S.A. Maloy, and A.M. Minor, *Nat. Mater.* 10, 608 (2011).
- M.D. Uchic, P.A. Shade, and D.M. Dimiduk, *JOM* 61, 36 (2009).
- D.E.J. Armstrong, A.S.M.A. Haseeb, S.G. Roberts, A.J. Wilkinson, and K. Bade, *Thin Solid Films* 520, 4369 (2012).
- D.E.J. Armstrong, M.E. Rogers, and S.G. Roberts, *Scr. Mater.* 61, 741 (2009).
- D. Di Maio and S.G. Roberts, *J. Mater. Res.* 20, 299 (2005).
- J.C. Gong and A.J. Wilkinson, *Acta Mater.* 57, 5693 (2009).
- S. Wurster, C. Motz, M. Jenko, and R. Pippan, *Adv. Eng. Mater.* 12, 61 (2010).
- J.C. Gong and A. Wilkinson, *Philos. Mag. Lett.* 90, 503 (2010).
- D.E.J. Armstrong, A.J. Wilkinson, and S.G. Roberts, *J. Mater. Res.* 24, 3268 (2009).
- D.E.J. Armstrong, A.J. Wilkinson, and S.G. Roberts, *Philos. Mag. Lett.* 91, 394 (2011).
- S. Wurster, C. Motz, and R. Pippan, *Philos. Mag.* 92, 1803 (2012).
- F. Iqbal, J. Ast, M. Goken, and K. Durst, *Acta Mater.* 60, 1193 (2012).
- B.N. Jaya, C. Kirchlechner, and G. Dehm, *J. Mater. Res.* 30, 686 (2015).
- P.R. Howie, S. Korte, and W.J. Clegg, *J. Mater. Res.* 27, 141 (2012).
- S. Korte and W.J. Clegg, *Scr. Mater.* 60, 807 (2009).
- S. Korte and W.J. Clegg, *Philos. Mag.* 91, 1150 (2011).
- F. Ostlund, P.R. Howie, R. Ghisleni, S. Korte, K. Leifer, W.J. Clegg, and J. Michler, *Philos. Mag.* 91, 1190 (2011).
- J.S.K.L. Gibson, S.G. Roberts, and D.E.J. Armstrong, *Mater. Sci. Eng. A* 625, 380 (2015).
- J.C. Trenkle, C.E. Packard, and C.A. Schuh, *Rev. Sci. Instrum.* 81, 073901 (2010).
- J.M. Wheeler, D.E.J. Armstrong, W. Heinz, and R. Schwaiger, *Curr. Opin. Solid State Mater. Sci.* (2015). doi:10.1016/j.cossms.2015.02.002.
- C.A. Schuh, C.E. Packard, and A.C. Lund, *J. Mater. Res.* 21, 725 (2006).
- A. Sawant, S. Tin, and J.C. Zhao, *Superalloys* (New York: Wiley, 2008), pp. 863–871.
- J.M. Wheeler, R.A. Oliver, and T.W. Clyne, *Diam. Relat. Mater.* 19, 1348 (2010).
- J.M. Wheeler and J. Michler, *Rev. Sci. Instrum.* 84, 045103 (2013).
- C. Walter, J.M. Wheeler, J.S. Barnard, R. Raghavan, S. Korte-Kerzel, P. Gille, J. Michler, and W.J. Clegg, *Acta Mater.* 61, 7189 (2013).
- N. Ono, K. Kitamura, K. Nakajima, and Y. Shimanuki, *Jpn. J. Appl. Phys.* 1, 368 (2000).
- P.B. Hirsch and S.G. Roberts, *Philos. Mag. A* 64, 55 (1991).
- S. Korte, J.S. Barnard, R.J. Steam, and W.J. Clegg, *Int. J. Plast.* 27, 1853 (2011).
- J. Rabier, A. Montagne, J.M. Wheeler, J.L. Demenet, J. Michler, and R. Ghisleni, *Phys. Status Solidi C* 10, 11 (2013).